Journal of Catalysis **211,** 157–164 (2002)
doi:10.1006/jcat.2002.3715

New Method of Measuring the Amount of Oxygen Storage/Release on Millisecond Time Scale on Planar Catalyst

Y. Sakamoto,*,[1] K. Kizaki,* T. Motohiro,* Y. Yokota,* H. Sobukawa, M. Uenishi,† H. Tanaka,† and M. Sugiura*

*Applied Catalysis Division, Toyota Central R&D Laboratories, Inc., Nagakute, Aichi 480-1192, Japan; and †Daihatsu Motor Co., Ltd., 1-1 Daihatsu-cho, Ikeda-shi, Osaka 563-8651, Japan

Received March 5, 2002; revised May 29, 2002; accepted June 10, 2002

A new method to measure the amount of oxygen storage in/release from catalysts on a millisecond scale per two CO pulses (MS-OSC) has been developed. The MS-OSC measurement is based on the principle of the fast detection of reaction products on catalyst surfaces just after CO and O_2 injections using pulsed valves by time-of-flight mass spectrometry. Each catalyst was slurry-coated on planar cordierite substrate. MS-OSC was measured under high-vacuum (10^{-7} Pa) conditions, which allowed the MS-OSC to be directly measured as the amount of CO_2 without diffusion effects. We applied the MS-OSC to the following three catalysts: Pt/CeO_2–ZrO_2 mixture, Pt/CeO_2–ZrO_2 solid solution, and Pt/CeO_2–ZrO_2–Y_2O_3 (Pt/CZY) solid solution. Pt/CZY was reported to improve the transient catalytic activity on a millisecond scale, which could not be explained by the result of conventional thermogravimetric OSC measurements on a second scale. From a comparison of the three catalysts, the MS-OSC of Pt/CZY was found to be the highest. This result is supported by a previously reported engine test result (H. Tanaka, I. Tan, K. Yamada, and M. Yamamoto, ASATA 98ATE018, 1998).

Key Words: **oxygen storage capacity; OSC; oxygen storage capacity in millisecond; MS-OSC; platinum; ceria–zirconia; ceria–zirconia–yttria; in vacuum; transient reaction.**

1. INTRODUCTION

Ceria is one of the most important materials for the automotive three-way catalyst reaction (TWCR) because of its oxygen storage/release capacity (OSC). OSC is usually defined as the amount of oxygen stored in and released from the catalysts (1–5). It is reported that the OSC could be significantly improved by the doping of Zr and Y into ceria (6–10). Recently, it was reported that the evaluation of $Pt/Ce_6Zr_3Y_{0.5}O_{19.5}$ by the mode-simulating dynamometer indicated a high catalytic activity (1). The doping of Y into ceria–zirconia solid solution could improve the transient catalytic activity that was closely related to the OSC, but the doping did not improve the OSC in this case. The result of a conventional OSC measurement did not support the engine tests (11). In a conventional measurement by a thermal gravimeter (TG), OSC is investigated on a time scale of seconds and its absolute quantity is usually described in weight. However, the exhaust-gas compositions in an engine tail pipe simultaneously change according to the engine operating cycle on a millisecond time scale. Therefore, the gases that pass through a catalytic converter closely coupled to engines are not under steady-state conditions but drastically change on a millisecond scale.

Only a limited number of studies have been presented on the OSC on a millisecond scale (12–14). If a microreactor system filled with pellet-type catalysts is used to measure the OSC as the standard catalytic reactivity measurement, the diffusion process, especially, the desorption process of the reaction products, spoils the time resolution of the products variation on the catalytic surface. Therefore, the results will not describe the exact features of the amount of oxygen storage in/release from catalysts on a millisecond scale (MS-OSC). On the other hand, the surface science approach, employing an ultrahigh vacuum and planar catalyst, is ideally suited for helping to understand surface phenomena because the complication due to diffusion process is negligible (15, 16). By employing this surface science approach in our newly developed apparatus (17), MS-OSC was measured with allows use to directly consider the MS-OSC as the amount of CO_2 without diffusion effects. The first objective of this study is to develop the MS-OSC measurement method of a catalyst on a planar substrate. The second objective is to investigate the relation between the MS-OSC and the other properties such as conventional OSC measurement, TWCR, Pt particle size, and support particle size.

2. EXPERIMENTAL

2.1. Catalyst Preparation

The CeO_2–ZrO_2 support, with the composition $CeO_2 : ZrO_2 = 1 : 1$ in molar ratio, was prepared by the

[1] To whom correspondence should be addressed. Fax: 81 561-63-6150. E-mail: sakamoto@mosk.tytlabs.co.jp.

0021-9517/02 $35.00

precipitation method in which aqueous ammonia was rapidly added to the solution of $Ce(NO_3)_3$ and $ZrO(NO_3)_2$ until the pH reached 10. The resulting precipitation was filtered, dried at 110°C overnight, and then calcined in air for 1 h at 500°C. The calcined support is denoted as the C_5Z_5 support. The CeO_2–ZrO_2–Y_2O_3 support of the composition, $CeO_2 : ZrO_2 : Y_2O_3 = 46.5 : 46.5 : 7.0$ in molar ratio, was prepared by the same method. The obtained support is denoted as $C_{46.5}Z_{46.5}Y_{7.0}$. The CeO_2–ZrO_2 support of the composition, $CeO_2 : ZrO_2 = 5 : 1$ in molar ratio, was prepared by the precipitation–impregnation method in which aqueous ammonia was rapidly added to the solution of CeO_2 powder and $Zr(NO_3)_2$ until the pH reached 10. The obtained support is denoted as C_5Z_1.

The Pt/C_5Z_1, Pt/C_5Z_5, and $Pt/C_{46.5}Z_{46.5}Y_{7.0}$ catalysts were prepared as follows. In a typical preparation, the C_5Z_5 support was impregnated with an aqueous nitrate solution of $Pt(NH_2)_2(NO_2)_2$, followed by calcining at 250°C for 1 h in air, and then cooling to 25°C to prepare the Pt/C_5Z_5 powdered catalyst. The Pt/C_5Z_5 and $Pt/C_{46.5}Z_{46.5}Y_{7.0}$ powdered catalysts were prepared using the same method. The Pt loading amount was 0.1 wt% for the catalysts.

A slurry was prepared by adding the powdered catalyst to deionized water and then reducing the amount of water by evaporation. The obtained slurry was wash-coated onto a planar cordierite substrate (50 mm × 50 mm × 1 t) and then dried at 110°C for 1 h to obtain the fresh planar catalysts for MS-OSC.

The powdered catalysts were pressed, crushed, and then sieved to form 0.3–0.7-mm pellets for the conventional measurement of the OSC and TWCR using the laboratory reactor. Some pellets and planar catalysts were heated at 1000°C for 2 h in the gas flow whose composition was changed from 1% O_2/N_2 to 1% H_2/N_2, and vice versa, every 5 min to obtain the thermally aged catalysts.

To investigate the influence of the H_2 reduction on fresh and aged planar catalysts, the catalysts were heated in a gas flow composed of 5% H_2/N_2 at 500°C for 1 h to obtain the H_2-reduced planar catalysts.

To investigate the influence of the amount of Pt in the $Pt/C_{46.5}Z_{46.5}Y_{7.0}$ catalyst on MS-OSC, fresh and aged planar catalysts with compositions of 0.01, 0.1, and 1.0 wt% $Pt/C_{46.5}Z_{46.5}Y_{7.0}$ were prepared using the same method as mentioned earlier.

To investigate the influence of support deterioration, Pt thin-film catalysts of about 5-nm thickness were sputter-deposited on planar cordierite substrates.

2.2. MS-OSC Measurement

Figure 1 shows a schematic of the apparatus to measure MS-OSC (16, 17). It consists of three pumped chambers. The interior of the chambers is kept at a high vacuum: the first chamber at about 10^{-6} Pa, the second chamber at $\sim 10^{-7}$ Pa, and the third chamber at $\sim 10^{-8}$ Pa. A planar-catalyst holder and four gas-pulsed valves are arranged in the first chamber to inject the feed gas on the planar catalyst. The measurement procedure of the MS-OSC measurement is indicated as follows. Each catalyst was placed in the first chamber as shown in Fig. 1. The reaction products emitted from the catalyst were sampled through a skimmer located in a direction normal to the catalyst plane. The extracted reaction product beam, which was collimated by the pass through the second chamber ($\sim 10^{-7}$ Pa), finally entered into the electron impact ionizer of the time-of-flight (TOF) mass spectrometer in the third chamber (10^{-8} Pa). The ionized reaction products were detected by the TOF mass spectrometer on a millisecond scale.

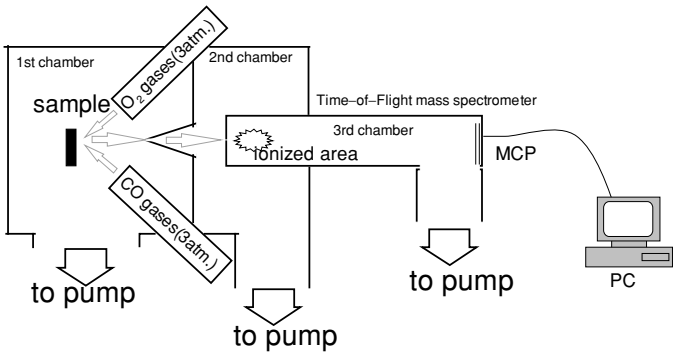

FIG. 1. Schematic of the apparatus used to measure MS-OSC.

Figure 2 shows the time profile of the average of 30 measurements for a pulsed gas (charged with 3 kg/cm^2 O_2, operated for 1.0, 1.5, 2.0, 2.5, and 3.0 ms of open time of the pulsed valve) reflected from the inert model catalyst of a fused silica plate (50 mm × 50 mm × 1 t) after the gas injection. When the open times were shorter than 0.5 ms, they were found to make sufficiently narrow initial fast profiles. After the gas injection, the pressure of each chamber rose

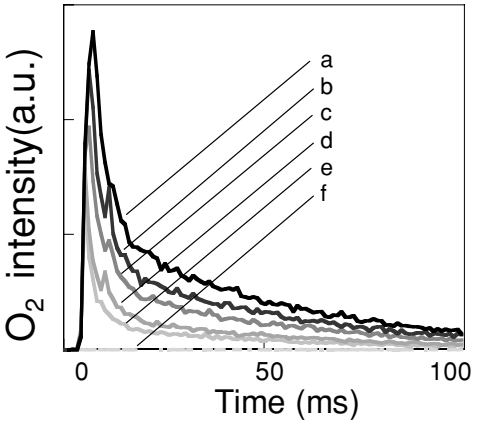

FIG. 2. O_2 emission profiles of a planar quartz sample after O_2 pulse injection. The open time of the O_2 pulse valve is indicated as follows: (a) 3.0 (b) 2.5 (c) 2.0 (d)1.5 (e) 1.0, and (f) 0.0 ms.

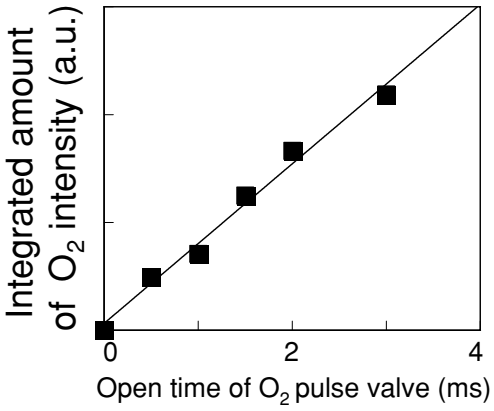

FIG. 3. Integrated amount of O_2 intensity in Fig. 2 as a function of open time of O_2 pulse valve.

quickly, but within 5 s it returned to the base pressure. The pulse width of the pulsed gas became greater than that of the corresponding open time of the pulsed valve, because these shapes were measured as the reflections from the surface of the planar catalyst. Figure 3 shows the integrated amount of O_2 intensity in Fig. 2 as a function of the detecting time. As shown in Fig. 3, the pulse width of O_2 was in proportion to the integrated amount of O_2. The amount of each O_2 pulse injection was about 0.1 cc when the pulse width was set at 1 ms.

Figure 4 shows the procedure for MS-OSC measurement. The surface temperature of all the planar catalysts was kept at 270°C for all MS-OSC measurements. As a pretreatment, CO was supplied to the surface of the planar catalysts until no more CO_2 was observed. After the pretreatment, the pulsed O_2 was supplied to the catalyst. The open time of the pulsed valve to inject O_2 was 0.3 to 4.0 ms. After 5 s, the pulsed CO, whose open time was set to 2.0 ms for the pulsed valve to inject CO, was supplied twice to the planar catalyst. CO reacted with the O_2 stored and adsorbed in the catalyst to form CO_2; the formed CO_2 was released from the catalyst. This procedure was repeated 30 times to improve the signal-to-noise ratio. The integrated amount of CO_2 per two CO pulses intensity released from the planar catalyst is defined as MS-OSC.

Another experiment concerning MS-OSC was done using the same procedure except that H_2 was pulsed instead of CO and that the temperature of the catalyst was 500°C.

2.3. Conventional OSC Measurement

Figure 5 shows the method for the conventional measurement of the OSC using a TG. The pellet catalyst was first exposed to a feed stream of 50% O_2/N_2 at 500°C for 4 min. The catalyst was then exposed to 20% H_2/N_2 at 500°C. In this process oxygen atoms that were stored in the reactor with H_2 form H_2O, which thus causes a weight loss of the catalyst. By measuring the weight loss, the evaluated amount of oxygen atoms from the catalyst was calculated to obtain the OSC.

2.4. Three-Way Catalyst Reactivity Measurement

To investigate the TWCR for each light-off test, thermally aged catalysts were evaluated using a previously

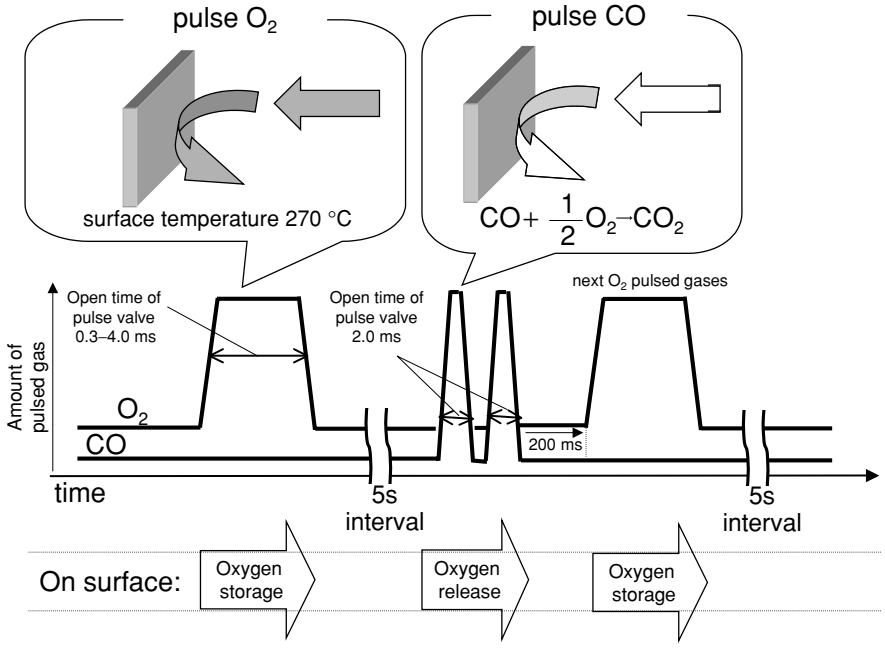

FIG. 4. Procedures for MS-OSC measurement.

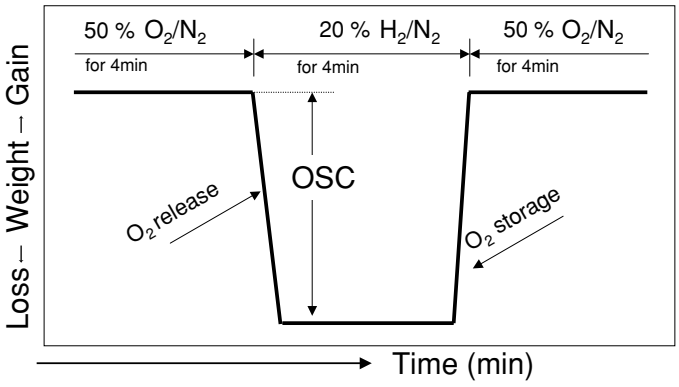

FIG. 5. Conventional OSC measurement by TG apparatus.

developed laboratory reactor (18). The catalytic activity data were obtained using a conventional fixed-bed flow reactor at atmospheric pressure. A quartz tube with an inner diameter of 18 mm was chosen as the reactor tube. A 1-cm^3-pellet catalyst was placed at the middle part of the reactor. The upper part of the catalyst bed was packed with 7 cm^3 of inactive SiC beads (3-mm o.d. in size) for preheating the atmosphere. The gas leaving the reactor was introduced into a condenser to remove the water vapor. The remaining components were continuously analyzed by several means: nondispersive infrared spectrometry for CO and CO_2, flame ionization for hydrocarbons (HC), magnetic susceptibility for O_2, and chemiluminesence for NO_x. They were all attached to a Horiba MEXA-8120 gas analyzer.

The atmosphere compositions and reaction conditions used in this study were as follows. The simulated stoichiometric mixture (simulated exhaust gas) consisted of 10.0% CO_2, 0.70% CO, 0.23% H_2, 1600 ppm C_3H_6, 1200 ppm NO, 0.64% O_2, 3 vol% H_2O, and the balance of N_2. This mixture simulates the stoichiometric ratio of air to fuel (A/F = 14.6). The evaluation atmosphere was periodically changed every 2 s around the stoichiometric atmosphere with a 4% A/F (from A/F = 14.0 to 15.2) amplitude, which is defined as the difference from the evaluation atmosphere to the stoichiometric atmosphere. This amplitude was produced by additional O_2 or $[3CO + H_2]$ injection (19). Catalysts were exposed to the simulated exhaust gas at 3.3 l/min while the temperature was decreased from 500 to 100°C at the rate of 5°C/min and the space velocity was about 200,000 h^{-1}. The conversion data were measured at temperatures from 500 to 100°C. The TWCR was expressed as the temperature at 50% conversion of NO, CO, and HC.

2.5. Measurement of Pt and Support Particle Sizes and Surface Area of the Catalyst

To determine the particle size of the Pt and support, the XRD measurement was carried out using a RIGAKU RU-3L X-ray diffractometer with Co $K\alpha$ radiation. The particle sizes were calculated using Sherrer's equation (20). The surface area of the catalysts was measured by the BET method with N_2 adsorption.

3. RESULTS

3.1. MS-OSC

Figures 6a, 6b and 6c show the time profile of the transient CO_2 production from the aged 0.1 wt% Pt/C_5Z_1, Pt/C_5Z_5, and $Pt/C_{46.5}Z_{46.5}Y_{7.0}$ catalysts, respectively, by sequential injections of CO and O_2 pulses. The temperature of these catalysts was 270°C. The CO pulsed gas was supplied to the catalyst at 0 and 100 ms. O_2 stored in the catalyst was

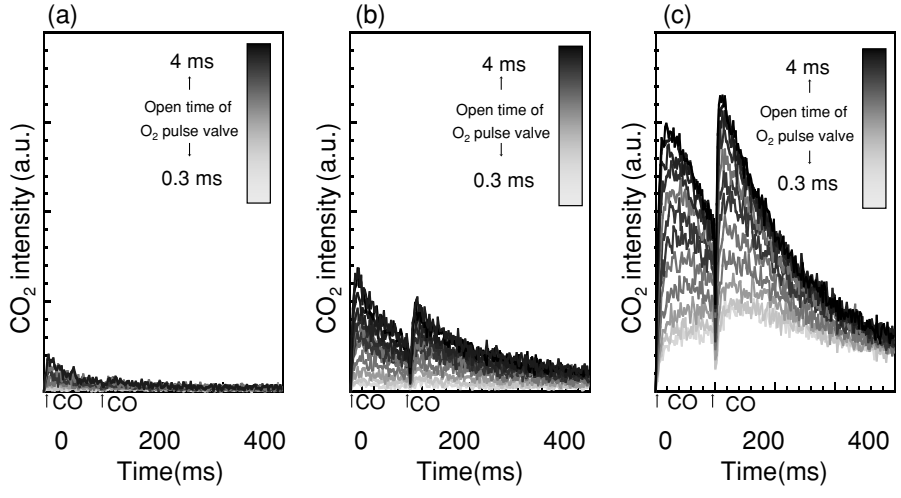

FIG. 6. Transient CO_2 production from aged 0.1 wt% Pt/C_5Z_1, Pt/C_5Z_5, and $Pt/C_{46.5}Z_{46.5}Y_{7.0}$ planar catalysts by sequential injection of two CO pulses as indicated by the two arrows: (a) 0.1 wt% Pt/C_5Z_1 (b) 0.1 wt% Pt/C_5Z_5, and (c) 0.1 wt% $Pt/C_{46.5}Z_{46.5}Y_{7.0}$ catalysts.

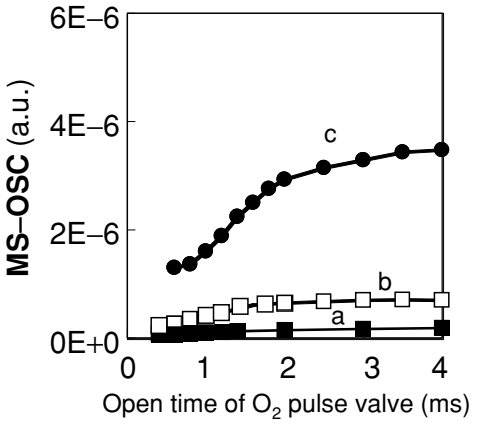

FIG. 7. MS-OSC (integrated amount of CO_2 per two CO pulses in Fig. 6) of aged 0.1 wt% $Pt/C_{46.5}Z_{46.5}Y_{7.0}$, Pt/C_5Z_5, and Pt/C_5Z_1 planar catalysts as a function of open time of O_2 pulse value: (a) $Pt/C_{46.5}Z_{46.5}Y_{7.0}$ (b) Pt/C_5Z_5, and (c) Pt/C_5Z_1.

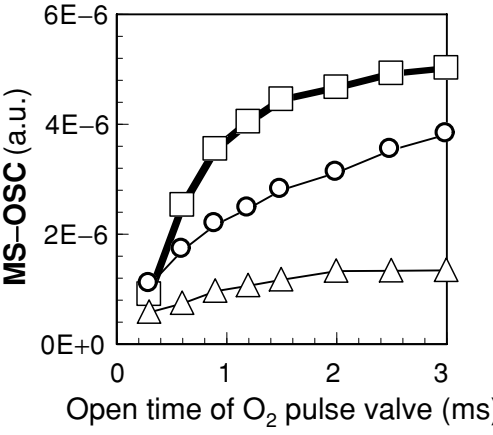

FIG. 9. Effect of Pt amount on MS-OSC of fresh $Pt/C_{46.5}Z_{46.5}Y_{7.0}$ catalysts: △, 0.01 wt% Pt; ○, 0.1 wt% Pt; and □, 1.0 wt% Pt.

released as CO_2 when the CO gases were supplied to the catalysts. Comparing these three catalysts, it was found that the greatest amount of CO_2 was released from the $Pt/C_{46.5}Z_{46.5}Y_{7.0}$ catalyst thus indicating the highest activity.

Figure 7 shows the MS-OSC (the integrated amount of CO_2 per two CO pulses in Fig. 6) for the three kinds of catalysts as a function of the open time of the O_2 pulse valve. The integrated amount of CO_2 roughly corresponds to that of O_2 as shown in Fig. 3. Therefore, the amount of generated CO_2 was found to be proportional to the amount of O_2 stored on the catalysts.

Figures 8a and 8b, respectively, show the MS-OSC of the fresh and aged 0.1 wt% $Pt/C_{46.5}Z_{46.5}Y_{7.0}$ and 0.1 wt% Pt/C_5Z_5 catalysts before and after heating in flowing 5% H_2/N_2 gas at 500°C for 1 h. H_2 reduction for the fresh catalyst was found to increase with the intensity of MS-OSC. On the other hand, H_2 reduction for the aged catalyst was less closely related to the increasing amount of MS-OSC.

Figure 9 shows the MS-OSC of fresh 0.01, 0.1, and 1.0 wt% $Pt/C_{46.5}Z_{46.5}Y_{7.0}$ catalysts. The MS-OSC of the catalysts was increased with increasing amount of Pt.

Figures 10a and 10b, respectively, show the MS-OSC of the catalysts consisting of the $C_{46.5}Z_{46.5}Y_{7.0}$ and C_5Z_5 support and Pt thin film deposited on it up to 5 mm in thickness, before and after the heat treatment at 500°C in the flowing gas of 5% H_2/N_2. Here, the interfacial area between Pt and the support remained unchanged for each catalyst, because the same amount of Pt was evaporated on each support by

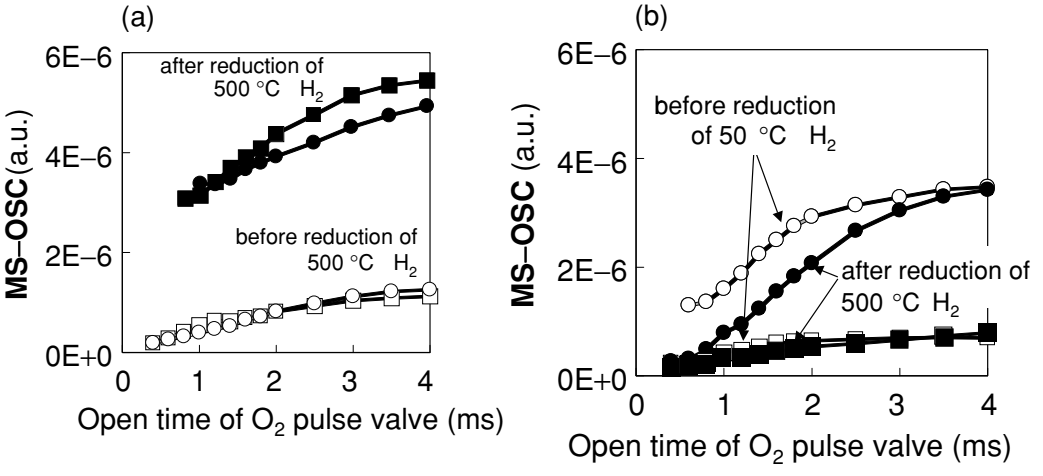

FIG. 8. MS-OSC of (a) fresh and (b) aged $Pt/C_{46.5}Z_{46.5}Y_{7.0}$ and Pt/C_5Z_5 planar catalysts before and after H_2 reduction at 500°C as a function of pulse width (open time of oxygen pulse valve). Aged catalysts are obtained by heating fresh catalysts at 1000°C: ○, 0.1 wt% $Pt/C_{46.5}Z_{46.5}Y_{7.0}$ planar catalysts before H_2 reduction at 500°C; □, 0.1 wt% Pt/C_5Z_5 planar catalyst before H_2 reduction at 500°C; ●, 0.1 wt% $Pt/C_{46.5}Z_{46.5}Y_{7.0}$ planar catalysts after H_2 reduction at 500°C; and ■, 0.1 wt% Pt/C_5Z_5 planar catalyst after H_2 reduction at 500°C.

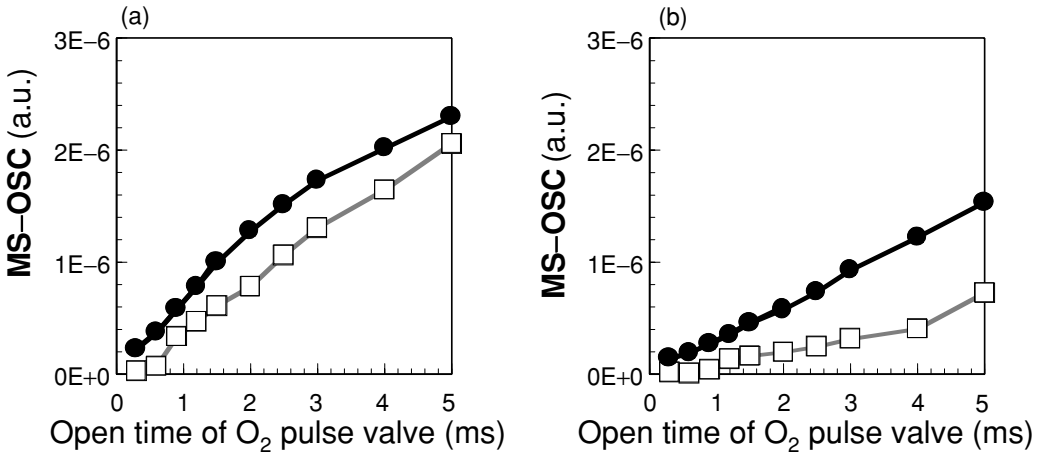

FIG. 10. MS-OSC of catalyst consisted of a sputter-deposited Pt thin film in 5-nm thickness on $C_{46.5}Z_{46.5}Y_{7.0}$ and C_5Z_5 supports (a) before and (b) after heated at 500°C in flowing 5% H_2/N_2: ●, 0.1 wt% Pt/$C_{46.5}Z_{46.5}Y_{7.0}$ planar catalysts; and □, 0.1 wt% Pt/C_5Z_5 planar catalyst.

the sputter method (20). Initially, both catalysts showed almost the same MS-OSC as shown in Fig. 10a; however, after the heat treatment of the support itself, the MS-OSC of the catalyst on the $C_{46.5}Z_{46.5}Y_{7.0}$ support was greater than that on the C_5Z_5 support as shown in Fig. 10b.

3.2. Conventional OSC

Figure 11 shows the conventional OSC of the aged 0.1 wt% Pt/C_5Z_1, 0.1 wt% Pt/C_5Z_5, and 0.1 wt% Pt/$C_{46.5}Z_{46.5}Y_{7.0}$ pellet catalysts. The OSC of the Pt/C_5Z_5 pellet catalyst was the greatest among these three catalysts.

3.3. Catalytic Activity

Figure 12 shows the temperature at 50% conversion (T50) of NO, CO, and HC on the aged 0.1 wt% Pt/C_5Z_5 and 0.1 wt% Pt/$C_{46.5}Z_{46.5}Y_{7.0}$ pellet catalysts. The aged Pt/$C_{46.5}Z_{46.5}Y_{7.0}$ catalyst was found to have a lower T50 indicating a higher TWCR than that of the Pt/C_5Z_5 catalyst.

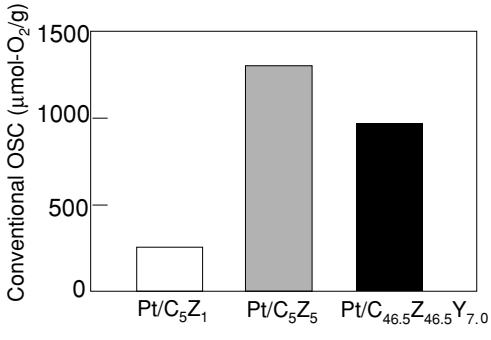

FIG. 11. Conventional OSC of aged pellet catalysts.

3.4. The Particle Size of Pt and Support and Surface Area

Figures 13a and 13b, respectively, show the particle size of the supports and Pt particles of the aged 0.1 wt% Pt/$C_{46.5}Z_{46.5}Y_{7.0}$ and 0.1 wt% Pt/C_5Z_5 powdered catalysts. The support particle size of the aged 0.1 wt% Pt/$C_{46.5}Z_{46.5}Y_{7.0}$ catalyst was greater than that of the aged Pt/C_5Z_5 catalyst as shown in Fig. 13a. However, the Pt particle size of the Pt/$C_{46.5}Z_{46.5}Y_{7.0}$ catalyst was smaller than that of the Pt/C_5Z_5 catalyst as shown in Fig. 13b. The Pt crystallite of the aged Pt/$C_{46.5}Z_{46.5}Y_{7.0}$ catalyst was so small that a Pt diffraction line could not be detected. Fig. 13c shows the surface area of the 0.1 wt% Pt/$C_{46.5}Z_{46.5}Y_{7.0}$ and 0.1 wt% Pt/C_5Z_5 powdered catalysts. The surface area of Pt/$C_{46.5}Z_{46.5}Y_{7.0}$ was higher than the one for Pt/C_5Z_5 in both the fresh and aged catalysts.

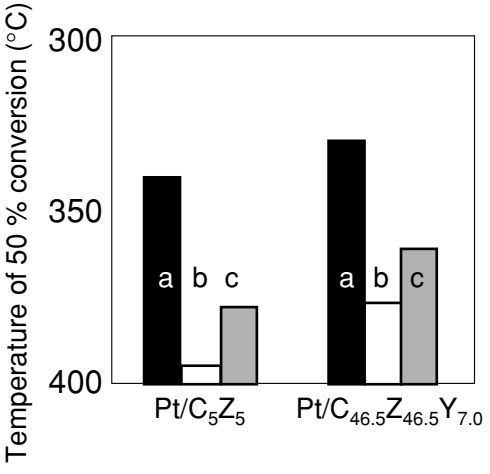

FIG. 12. Temperature at 50% conversion of NO, CO, and HC for aged pellet catalysts with 0.1 wt% Pt heated at 1000°C: (a) NO, (b) CO, and (c) HC.

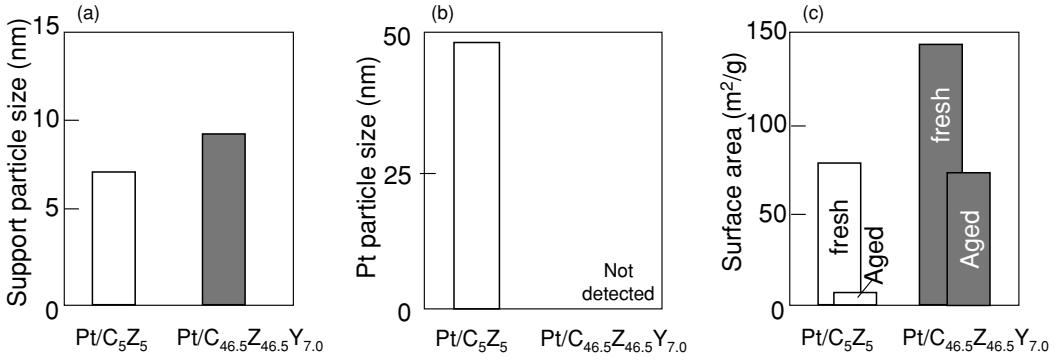

FIG. 13. Mean particle size for aged powdered catalysts and surface area for fresh and aged powders: (a) support particle size (b) Pt particle size, and (c) surface area.

4. DISCUSSION

To determine the best conditions where the OSC of ceria is fully utilized in the automotive catalyst, it is important to understand the OSC phenomenon on a millisecond time scale. Oxygen storage was considered to occur very fast not only on the Pt-catalyzed ceria but also on pure ceria, whereas the oxygen release was considered to be slow (21). In particular, the response of oxygen release toward the pulsed CO must be connected to the limiting factor for the purification of exhaust gases from an automobile. The intensity of the MS-OSC signal is the response of O_2 release at CO pulses. The result obtained in this study corresponded to the results of other measurements such as the TWCR (Fig. 12), Pt particle size (Fig. 13b) and also the result of engine tests (11). Therefore, MS-OSC is thought to be a suitable measure for comparing the OSC in real engine emissions.

The wash-coat thickness of all samples was measured to be almost 500 μm. It was roughly estimated that the ratio of the amount of oxygen storage and release to the total amount of OSC measured by a conventional method was about $\frac{1}{100} - \frac{1}{1000}$. The oxygen storage and release reaction was considered to occur at the surface. Surface roughness may affect MS-OSC on the surface. Figure 13c indicated that the surface area of the fresh $Pt/C_{46.5}Z_{46.5}Y_{7.0}$ was almost two times greater than that of the fresh Pt/C_5Z_5. However, MS-OSC of these samples was almost the same (Fig. 8a); nevertheless, the Pt particle size on both supports was very small. It was considered that the surface roughness factor must be a minor condition in these cases.

Here, the cause of the $C_{46.5}Z_{46.5}Y_{7.0}$ catalyst being thermally more stable than the Pt/C_5Z_5 catalyst is discussed. The loss of OSC is caused by several factors: growth of the particle size of CeO_2 (22, 23), loss in surface area of CeO_2 (24, 25), structure changes in the oxides (26, 27), and loss of contact force between the precious metal and CeO_2 (8, 28, 29). Also, the addition of ZrO_2 to CeO_2 and Y_2O_3 leads to an improvement in the OSC (8, 30–32). The thermal stability prevents the loss in surface area of the $C_{46.5}Z_{46.5}Y_{7.0}$ and Pt particles sintering on $C_{46.5}Z_{46.5}Y_{7.0}$. On the other hand, the intensity of the MS-OSC signal is found to depend significantly on the physical state of the Pt particles. The intensity of MS-OSC signal becomes higher as shown in Figs. 6 and 9 for the following cases: when the size of the Pt particles becomes small (Figs. 7 and 13b), and when the amount of pulsed oxygen is increased (Figs. 6 and 9). The loss of the MS-OSC signal intensity should be caused mainly by the poor interface between the Pt particle and ceria component. Figure 10 shows another cause of the loss of MS-OSC intensity. The amount of Pt and particle size of the $Pt/C_{46.5}Z_{46.5}Y_{7.0}$ and Pt/C_5Z_5 catalysts are supposed to be almost the same (20). However, the intensity of CO_2 in the MS-OSC measurement for the $Pt/C_{46.5}Z_{46.5}Y_{7.0}$ catalyst was higher than that of the Pt/C_5Z_5 catalyst. This result is responsible for the exact cause as to the why $C_{46.5}Z_{46.5}Y_{7.0}$ support may be thermally more stable than the C_5Z_5 support.

5. CONCLUSIONS

The faster response of the OSC plays a more important role than the slower response of the conventional OSC on three-way catalysts to purify exhaust gases under transient atmosphere in a real engine. We have developed a new method to measure the fast response of the OSC, which we call the MS-OSC method. By measuring the MS-OSC, the following results were obtained:

1. The MS-OSC measurement is based on the principle of the fast detection of reaction products on catalyst surfaces following CO and O_2 injections using pulsed valves by TOF mass spectrometry.
2. MS-OSC is regarded as the response of CO_2 released from the catalyst by CO pulsed on a millisecond scale.
3. MS-OSC significantly depends on the Pt particle size of the Pt catalyst with the ceria component.
4. MS-OSC is in good agreement with the engine test results (11).

REFERENCES

1. Taylor, K. C., *Catal. Rev. Sci. Eng.* **35**, 457 (1993).
2. Gandhi, H. S., Piken, A. G., Shelef, M., and Delosh, R. G., SAE Paper 760201 (1976).
3. Schlatter, J., SAE Paper 780199 (1978).
4. Yao, H. C., and Yao, Y. F. Y., *J. Catal.* **86**, 254 (1984).
5. Fisher, G. B., Thesis, J. R., Casarella, M. V., and Mahan, S. T., SAE Paper 931034 (1993).
6. Miyoshi, N., Matsumoto, S., Ozawa, M., and Kimura, M., SAE Paper 891970 (1989).
7. Ozawa, M., Kimura, M., and Isogai, A., *J. Alloys Compd.* **193**, 73 (1993).
8. Matsumoto, S., Miyoshi, N., Kanazawa, T., Kimura, M., and Ozawa, M., *in* "Catal. Sci. and Tech." (S. Yoshida, N. Tabezawa, and T. Ono, Eds.), Vol. 1, p. 335. Kodansha-VCH, 1991.
9. Yamada, K., Tanaka, H., Aozasa, A., Matui, H., and Motoyama, M., *J. Alloys Comp.* **193**, 298 (1993).
10. Suda, A., Sobukawa, H., Suzuki, T., Kandori, T., Ukyo, Y., and Sugiura, M., *J. Ceram. Soc.* **109**, 177 (2001).
11. Tanaka, H., Tan, I., Yamada, K., and Yamamoto, M., ASATA 98ATE018 (1998).
12. Vidal, H., Bernal, S., Kašpar, J., Pijolat, M., Perrichon, V., Blanco, G., Pintado, J. M., Baker, R. T., Colon, G., and Fally, F., *Catal. Today* **54**, 93 (1999).
13. Nibbelke, R. H., Nievergerd, A. J. L., Hoebink, J. H. B. J., and Marin, G. B., *Appl. Catal*., *B* **19**, 245 (1998).
14. Holmgen, A., and Anderson, B., *J. Catal.* **178**, 14 (1998).
15. Altman, E. I., and Gorte, R. J., *Surf. Sci.* **195**, 392 (1988).
16. Motohiro, T., Kizaki, Y., Sakamoto, Y., Higuchi, K., Tanabe, T., Takahashi, N., Yokota, Y., Doi, H., Sugiura, M., and Noda, S., *Appl. Surf. Sci.* **121/122**, 323 (1997).
17. Motohiro, T., Kizaki, Y., Sakamoto, Y., Higuchi, K., Watanabe, Y., and Noda, S., *Appl. Surf. Sci.* **121/122**, 319 (1997).
18. Muraki, H., Yokota, K., and Fujitani, Y., *Appl. Catal.* **48**, 93 (1989).
19. Shinjoh, H., Takahashi, N., Yokota, K., and Sugiura, M., *Appl. Catal.*, *B* **15**, 189 (1989).
20. Cullity, B. D., *in* "Elements of X-ray Diffraction" (M. Cohen, Ed.), 2nd ed., p. 285. Addison–Wesley, Reading, MA, 1987.
21. Holmgren, A., and Andersson, B., *J. Catal.* **178**, 14 (1998).
22. Cordatos, H., Bunluesin, T., Stubeenrauch, J., Vohs, J. M., and Gorte, R. J., *J. Phys. Chem.* **100**, 785 (1996).
23. Zhang, Y., Anderson, S., and Muhammaed, M., *Appl. Catal.*, *B* **6**, 325 (1995).
24. Hakonen, M. A., Aita, E., Lahtl, A., Luoma, M., and Maunula, T., SAE paper 910846 (1991).
25. Trovarelli, A., deLeitenburg, C., DolCetti, G., and Lorca, J. L., *J. Catal.* **151**, 111 (1995).
26. Bunluesin, T., Cordatos, H., and Gorte, R. J., *J.Catal.* **157**, 222 (1995).
27. Bunluesin, T., Grorte, R. J., and Graham, G. W., *Appl. Catal.*, *B* **14**, 105 (1997).
28. Nunan, J. G., Robota, H. J., Cohn, M. J., and Bradley, S. A., *J. Catal.* **133**, 309 (1992).
29. Kalakkad, D. S., Datye, A. K., and Robota, H. J., *J.Catal.* **148**, 729 (1994).
30. Hori, C. E., Permana, H., Simon Ng, K. Y., Brenner, A., More, K., Rahmoeller, K. M., and Belton, D., *Appl. Catal.*, *B* **16**, 105 (1998).
31. Murata, T., Hasegawa, T., Aozasa, S., Matsui, H., and Motoyama, M., *J. Alloys Compd.* **193**, 298 (1993).
32. Fornasiero, P., Monti, R. D., Rao, G. R., Kaspar, J., Meriani, S., Trovarelli, A., and Graziani, M., *J. Catal.* **151**, 168 (1995).